THE JOURNAL OF PHYSICAL CHEMISTRY B

Article

pubs.acs.org/JPCB

Supramolecular Polymerization: A Coarse Grained Molecular Dynamics Study

Karteek K. Bejagam and Sundaram Balasubramanian*

Chemistry and Physics of Materials Unit, Jawaharlal Nehru Centre for Advanced Scientific Research, Bangalore 560 064, India

Supporting Information

ABSTRACT: A coarse-grained (CG) force field to model the self-assembly of benzene-1,3,5-tricarboxamide (BTA) class of compounds in nonpolar solvents has been developed. The model includes an intrinsic point dipole embedded on one of the CG beads so as to impart a macrodipole moment to the oligomer, one of its characteristic feature. Chemical specificity has been preserved by benchmarking against results, including dimerization and solvation free energies, obtained from an all-atom representation. Starting from a well-dispersed configuration in *n*-nonane, BTA molecules self-assemble to form one-dimensional stacks. Free energy (FE) changes for the various manner in which short oligomers can exchange between the assembled and the dispersed states have been calculated. These calculations show BTA to self-assemble via a downhill cooperative mechanism with a nucleus size of three.

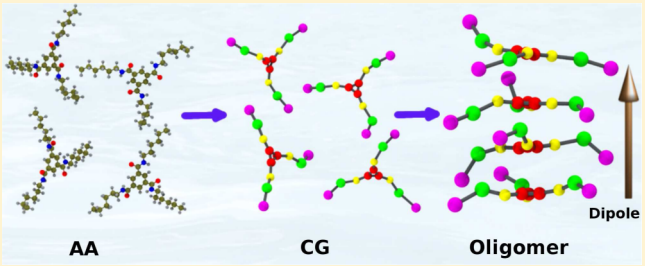

INTRODUCTION

Supramolecular polymers have been well studied through a variety of experiments due to their vital importance in optoelectronic[1] and biomedical applications.[2] Among them, benzene-1,3,5-tricarboxamide (BTA) is one of the most widely studied molecules as it readily self-assembles into one-dimensional, 3-fold hydrogen bonded stacks in nonpolar solvents.[2−4] Aggregation of these molecules proceeds in a cooperative fashion.[5,6] The oligomers possess a macrodipole moment along the stacking direction[7] whose magnitude increases with oligomer size. Interactions between oligomers are dominated by long-range dipole−dipole interactions, which is correlated with the cooperative nature of self-assembly.[8] Different phases of BTA and its derivatives have been explored in solid-state,[9,10] liquid-crystalline[11,12] and solution phases[13,14] experimentally. BTA with amino acids on their peripheries has been shown to self-assemble in the ionic liquid media.[15] BTA nanofibers have been used as a template for the controlled growth of gold nanoparticles.[16] Computational studies include the determination of oligomer structure,[6,17,18] dynamics of self-assembly, cooperativity in binding energies, and free energies.[7]

A solution of achiral BTA molecules contains oligomers of P and M enantiomers in equal amounts.[3] However, the presence of a stereogenic center will offer a bias to handedness, giving rise to a net Cotton effect. Furthermore, the position of the stereocenter on the alkyl tail will determine the sign of the circular dichroism (CD) signal.[19] The shape of the solvent molecules (linear or cyclic) has also been shown to play an important role in determining the details of the CD spectrum,[19,20] and the same was attributed to the difference in the amide conformation with respect to the benzene core. Probing these observations at a microscopic level is experimentally challenging; however, molecular dynamics (MD) simulations of realistic chemical models can provide much needed insights on these aspects.

In our earlier work on BTA,[7] we showed that the asymmetric stacking unit, one in which not all three hydrogen bond dipole vectors between two molecules in the stack are aligned, is more stable than the symmetric one. Quantum chemical calculations as well as all-atom empirical potential-based MD simulations at finite temperature unequivocally showed the asymmetric stack to be the ground state. However, studies of the self-assembly of such molecules in solution via realistic all-atom (AA) MD simulations are computationally challenging due to the large number of degrees of freedom, difficulties in sampling and the time scales involved. Fundamental questions on the mechanism of self-assembly can be answered if models with fewer degrees of freedom are constructed. They could permit the study of the mechanism and thermodynamics of self-assembly from a microscopic perspective.

The main aim of the present work is to develop a coarse-grain (CG) model for BTA and employ the same to probe the mechanism of its self-assembly in a nonpolar solvent. Coarse-graining is a powerful tool that can be employed to access length and time scales that exist between atomistic and mesoscale simulations.[21] It is possible to build coarse grain models that reduce the number of degrees of freedom drastically, yet retain chemical specificity.[22−25] Furthermore, due to the softness of the interactions between CG beads, a larger time step can be used to integrate the equations of

Received: February 18, 2015
Revised: April 6, 2015
Published: April 8, 2015

DOI: 10.1021/acs.jpcb.5b01655
J. Phys. Chem. B 2015, 119, 5738−5746

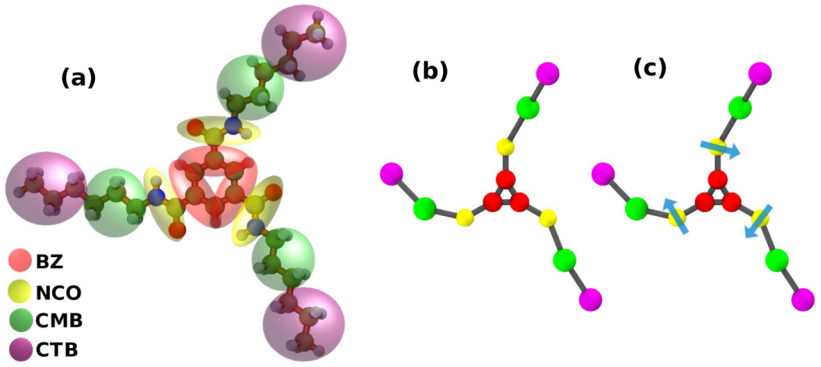

Figure 1. (a) Schematic representation of CG mapping on atomistic representation. CG representation of a monomer in (b) Model A and (c) Model B. Blue arrow represents the point dipole on the NCO bead.

motion. Self-assembled structures in various domains have been explored through CG models.[26−28] Following the approach of many researchers in the development of CG models,[29−32] the dimerization (DFE) and solvation (SFE) free energy profiles for BTA as determined from AA MD simulations[7] were used as benchmarks in developing the CG potentials here.

The mapping scheme and the systematic procedure adopted in developing two CG models will be presented in the next section. The self-assembly of BTA molecules in *n*-nonane solution is demonstrated later. Furthermore, free energy (FE) calculations are employed to explore the phenomenon underlying monomer exchange within the sergeants-and-soldiers principle.[33] Using free energy calculations, we observe that the self-assembling behavior can be characterized as downhill cooperative, and the critical nucleus is diagnosed to be a trimer.

METHODOLOGY AND SIMULATION DETAILS

Mapping Scheme. In the CG model, a set of atoms were grouped together to be represented by a single entity called a "bead". The mass and position of the bead were taken to be the sum of the masses of atoms and the center of mass of atoms constituting it, respectively. The benzene core of BTA was mapped onto three BZ beads, and each amide was represented by a NCO bead. The mapping of alkyl tails and solvent *n*-nonane was adopted from Shinoda et al.[30] Figure 1 describes the mapping scheme. Charge on the beads was evaluated as described in Supporting Information (see Figure S1). We call this model "Model A". Through this approach, a BTA molecule with three hexyl tails consisting of 78 atoms can be represented by just 12 beads. A CG representation of BTA has four atom types. With this mapping scheme, and with the bead−bead interaction parameters determined through benchmarks against AA simulations, the model was able to exhibit self-assembly (*vide infra*); however, a crucial feature of oligomers modeled within the atomistic approach is the development of a macrodipole along the stacking direction—one that is absent in the CG model developed above. Thus, it is crucial that a CG model be developed that possesses this feature. We call such a model "Model B".

Model B. In a single molecule of BTA in gas phase, the C═O and N−H bond vectors present in each branch are coplanar, and thus the molecule possesses zero net dipole moment. Upon oligomerization, hydrogen bonds are formed between amide groups of neighboring molecules. Thus, a dipole moment is generated for each hydrogen bond, which arises due to the fact that the N−H and C═O groups of a molecule are oriented normal to the benzene plane in either direction.[7] The dipole moment of every amide group adds up along the stacking direction, to result in a macrodipole for the stack. Note that there are three amide groups per molecule, and it has previously been shown by us that the 2:1 configuration, one in which the dipole vectors of only two amide groups are oriented parallel to each other, is more stable than the 3:0 configuration.[7] Model A described earlier lacks this dipole moment. In order to impart a dipole moment to the NCO bead, we have borrowed the idea of tagging a point dipole over an atom from the Stockmayer fluid model,[34,35] which has been effectively used in modeling liquid crystals. An intrinsic point dipole with moment 1.82 D was introduced to lie on each NCO bead (see Figure 1). Orsi[36,37] has developed CG models for water and lipids using a similar approach. Thus, in Model B, the nonbonded interactions include van der Waals (E_{LJ}), charge−charge (E_{qq}), dipole-point charge (E_{qp}) and dipole−dipole (E_{pp}).

Simulation Details. The intramolecular potential terms included bond and angle energy functions. Beads separated by more than two bonds interacted via a nonbonded potential. All beads were treated as point particles, the standard norm in atomistic MD simulations; the NCO beads in Model-B, however, had two attributes: a point-like feature for Lennard-Jones and electrostatic interactions and as a sphere for the rotational motion associated with the explicit dipole embedded on it. In addition to the charge, the NCO bead also possesses a point dipole vector (in Model B) whose magnitude was chosen so as to give a significant macrodipole (*vide infra*) along the stacking direction. All the point particles were coupled to a Nosé−Hoover thermostat.[38,39] For spherical particles, both the center of mass and dipole rotational degrees of freedom were coupled to a Langevin thermostat.[40] All the CGMD simulations were performed using LAMMPS.[41] A real space cutoff of 15 Å was used for the nonbonded interactions. Long-range Coulombic interactions were treated using particle−particle particle-mesh (PPPM) solver with an accuracy of 1×10^{-5}. A time step of 4.0 fs was used to integrate the equation of motions. Three-dimensional periodic boundary conditions were applied. FE calculations were performed using the collective variables module[42] integrated with LAMMPS. For both models, 9−6-type Lennard-Jones potential was employed for the nonbonded interactions. VMD[43] and JMOL[44] were used for visualizations. The nonbonded interactions are as follows:

DOI: 10.1021/acs.jpcb.5b01655
J. Phys. Chem. B 2015, 119, 5738−5746

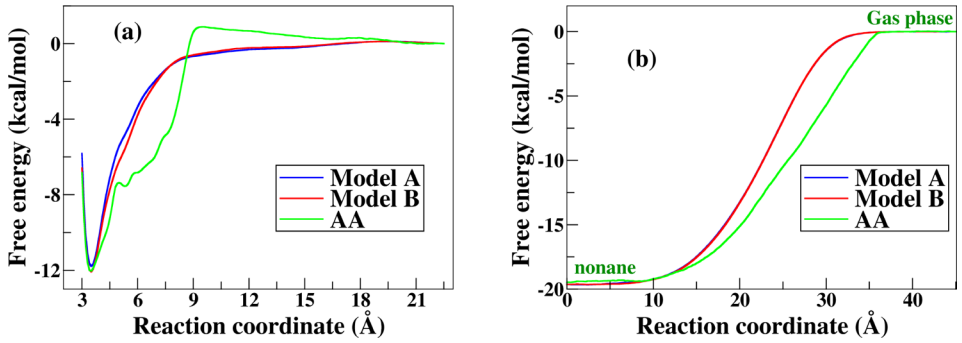

Figure 2. Comparison of the (a) dimerization and (b) solvation free energy profiles. AA: all-atom; Models A and B are CG representations.

$$
\begin{aligned}
E_{nb} &= E_{LJ} + E_{qq} + E_{qp} + E_{pp} \\
\text{where, } E_{LJ} &= \frac{27}{4}\epsilon\left[\left(\frac{\sigma}{r}\right)^9 - \left(\frac{\sigma}{r}\right)^6\right] \\
E_{qq} &= \frac{q_i q_j}{(4\pi\epsilon_o r_{ij})} \\
E_{qp} &= \frac{q}{r^3}(\vec{p}\cdot\vec{r}) \\
E_{pp} &= \frac{1}{r^3}(\vec{p_i}\cdot\vec{p_j}) - \frac{3}{r^5}(\vec{p_i}\cdot\vec{r})(\vec{p_j}\cdot\vec{r})
\end{aligned} \tag{1}
$$

Here, q and $\vec{p}$ represent charge and dipole on the bead, respectively.

PARAMETRIZATION OF CG POTENTIALS

Bonded Parameters. As mentioned earlier, beads separated by one and two bonds interacted via bond and angle potentials, respectively. In order to obtain these potentials, an AA simulation of one BTA molecule in gas phase was carried out at 298.15 K. From this trajectory, the positions of CG beads were identified as the center of mass of the corresponding atom group onto which they are mapped. Bond distance and angle distributions from this trajectory were used as the reference for the development of intramolecular CG potentials. Initial guesses for these intramolecular terms were obtained by a Boltzmann inversion of the bond and angle distributions (between bead centers) obtained from the reference AA MD simulations. These were refined multiple times until the distributions of bead−bead distances and angles obtained from the CG MD simulations of a monomer matched those from the AA MD simulations.

Intramolecular bond and angle distributions for beads associated with the alkyl tails can be bimodal due to their conformational flexibility. In our parametrization, bond and angle potentials were fitted to a harmonic form, where such distributions were unimodal, while bimodal distributions were reproduced using tabulated potentials as shown in Figure S2.

Nonbonded Parameters. The parametrization of nonbonded potentials was a more challenging task. Three sets of interactions—BTA−BTA, BTA−nonane, andnonane−nonane—were required. Nonane−nonane parameters were adopted from Shinoda et al.[30] Next, we were interested in obtaining the cross interactions between BTA and solvent beads. Toward this purpose, MD simulation of one AA BTA molecule soaked in a box of AA *n*-nonane was carried out at 298.15 K in the canonical (NVT) ensemble. The radial distribution functions (RDF) between the bead positions of BTA and nonane were obtained. The potential of mean force (PMF) between the beads was obtained as $-k_B T \ln(g(r))$. The PMF formed the initial guess for the interaction potentials. Analogous CGMD simulations were performed with this potential to compare the $g(r)$ against those obtained from the AA simulation. The nonbonded interaction parameters between BTA and nonane beads were refined iteratively until satisfactory agreement was obtained, as demonstrated in Figure S3. Parameters of Shinoda et al.[30] were found to be effective in describing the interactions between the alkyl tails of BTA and nonane and thus were employed as-is. In order to derive BTA−BTA interaction parameters, the procedure of matching RDF profiles in either its liquid state or in the solution state can lead to erroneous models of self-assembly. Thus, the dimerization and solvation free energy profiles of AA BTA in *n*-nonane, which were determined in our earlier work[7] were used as references to determine these interaction parameters for CG simulations.

As mentioned earlier, the NCO bead represents the amide group in AA representation, which has the capability of forming a hydrogen bond with the amide group of a neighboring molecule. The strength of one such hydrogen bond in a BTA dimer has previously been shown to be around 5 kcal/mol.[7] The AA model of BTA[7] included a specific hydrogen bond potential term that was not only short-ranged (typically less than 5 Å) but also possessed an orientation dependence; this short-range interaction needs to be incorporated in the CG model as well. In order to mimic such short-range hydrogen bond interactions, the NCO−NCO potential was split into two Lennard-Jones (9−6, see eq 1) terms, one with the default cutoff (15 Å) having smaller "ϵ" and a shorter-ranged one (5 Å cutoff) with a higher "ϵ" value. Adaptive biasing force (ABF)[45] simulations were repeatedly performed by refining the parameters of these nonbonded interactions until the dimerization and solvation free energy profiles obtained from the CGMD simulations matched with the corresponding AA ones. The same are shown in Figure 2, and the values are provided in Table 1.

Table 1. Dimerization (DFE) and Solvation (SFE) Free Energies (in kcal/mol) for AA and CG Models[a]

	DFE	SFE	$\pi-\pi$ distance
Model A	−11.79	−19.65	3.44
Model B	−12.07	−19.64	3.43
all-atom	−12.03	−19.47	3.52

[a]Last column is the intermolecular distance (in Å).

DOI: 10.1021/acs.jpcb.5b01655
J. Phys. Chem. B 2015, 119, 5738−5746

Stack Stability and Intermolecular Distance. CGMD simulations of a preformed BTA oligomer of size 20 were carried out in *n*-nonane solution at 298.15 K using both of the models. All $\pi-\pi$ contacts were found to be intact throughout the simulation duration of 10 ns; the stack structure was also found to be preserved. Thus, it can be inferred that the CG parameters developed here represent the system well. The distribution of intermolecular distances measured between benzene centers of neighboring molecules via the AA and CG models are shown in Figure 3. The mean values obtained from the CG distributions are in good agreement with those from AA and are summarized in Table 1.

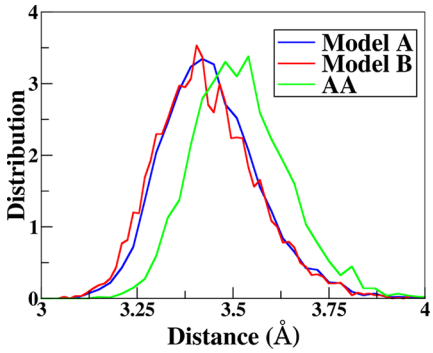

Figure 3. Distributions of intermolecular distances obtained from simulations of the preformed oligomer of size 20 in solvent.

Dipole Orientations. We have recently shown that the asymmetric stacking structure (2:1 hydrogen bonded) is more stable than a symmetric one (3:0 hydrogen bonded).[7] Representative dimers of these two configurations are shown in Figure 4a. A symmetric dimer, in which all the three hydrogen bond dipoles are parallel to each other, results in three "ferromagnetic-like" interactions, whereas in an asymmetric dimer, two h-bond dipoles are parallel to each other while the third is antiparallel to both, resulting in two "antiferromagnetic-like" and one "ferromagnetic-like" interactions. A preference for the 2:1 configuration was seen in the gas phase quantum chemical calculations as well as empirical force field-based AA MD simulations.[7] We were thus curious to see whether the CG model (Model B) will reproduce this feature. A CGMD simulation of a preformed decamer (initiated in 3:0 fashion) soaked in *n*-nonane was carried out at 298.15 K. Rotational degrees of freedom of dipoles were coupled to a Langevin thermostat as described before and were free to rotate. The dipoles were seen to rearrange themselves in an asymmetric (2:1) fashion within 1.5 ns and remained so thereafter for over 20 ns, as shown in Figure 4b, consistent with results from AA simulations.

Supramolecular Aggregation. Having compared the results of the CG MD simulations to those from AA MD, what remains to be verified is the process of self-assembly of BTA in solution, starting from a random initial configuration. Toward this end, an initial configuration of 30 monomers randomly dispersed in *n*-nonane solution was generated using Packmol.[46] MD simulations of the system was carried out at 298.15 K in the NPT ensemble using both the CG models A and B. The formation of smaller oligomers that later grew into larger ones was observed in both the models. Snapshots illustrating the self-assembly are provided in the Supporting Information (Figures S4 and S5). In Model B, due to the presence of an intrinsic point dipole, the oligomer possesses a macrodipole moment along the stacking direction. Since a macrodipole is an essential feature of BTA-based systems, all further analyses reported here have been carried out using Model B.

On the basis of a simulation of a system containing 10 BTA molecules in a solvent bath of 1000 *n*-nonane molecules, we observe a 400-fold improvement in the wall-clock time needed to generate a trajectory of the same duration (real-time) for the CG model over the AA one.

RESULTS AND DISCUSSION

Self-Assembly. Supramolecular polymerization of BTA proceeds spontaneously even at very dilute (μM) concentrations. In the previous section, self-assembly in a nonpolar solvent was demonstrated through both the CG models. While the concentration of BTA employed in experiments is in the range of micromolars, the same cannot be readily realized in simulations (even within a coarse grain approach) due to the computational challenges. A modest attempt is made herein, where we study the self-assembly of BTA at millimolar concentration. The simulation system contained 250 BTA

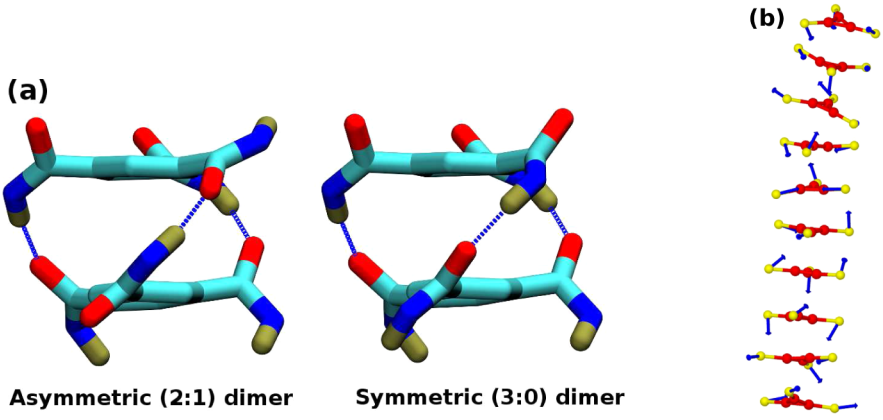

Figure 4. (a) Two possible configurations of BTA dimer in its AA representation.[7] Color scheme: carbon - cyan; hydrogen - tan; nitrogen - blue; oxygen - red. (b) Snapshot of a decamer, represented using Model B at 298.15 K in *n*-nonane, which prefers the asymmetric (2:1) configuration of dipole vectors. Thick arrows in blue represent the point dipole on NCO beads. CMB and CTB beads, as well as solvent molecules are not shown for clarity.

DOI: 10.1021/acs.jpcb.5b01655
J. Phys. Chem. B 2015, 119, 5738−5746

molecules dispersed in a bath of 200 000 *n*-nonane molecules, within a cubic box whose edge length is 40.0 nm corresponding to 6.03×10^5 CG beads in all. MD simulations were carried out in the canonical (NVT) ensemble at 298.15 K. BTA molecules were modeled using Model B as described above. Configurations were saved every 8 ps for postprocessing analysis. Snapshots showing the progress of self-assembly as a function of time are exhibited in Figure 5. Within a few tens of

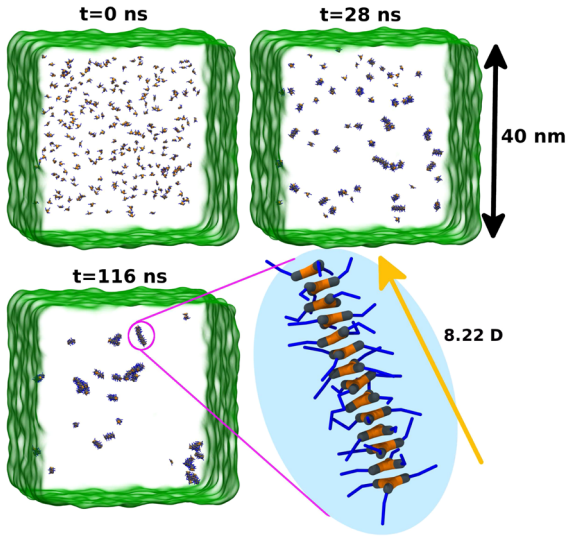

Figure 5. Snapshots illustrating the aggregation of 250 CG BTA molecules dispersed in 200 000 *n*-nonane molecules at 298.15 K, over time. A magnified view of one oligomer with its dipole vector of magnitude 8.22 D is also shown. Color scheme: BZ - orange; NCO - gray; CMB and CTB - blue. Nonane molecules are represented using the "QuickSurf" drawing method,[43] which is why they are not explicitly shown. Point dipoles on NCO beads are not shown for clarity.

nanoseconds, monomers coalesce to form smaller oligomers, and these elongate into longer oligomers over hundreds of nanoseconds. One such oligomer containing 14 molecules is highlighted in Figure 5 for a clear visualization. The macro-dipole moment of an oligomer was determined as $\sum(q_i \times r_i) + \sum\vec{p}_i$, where q_i and r_i are the charge and position of bead i, respectively, while $\vec{p}_i$ is the point dipole of the NCO bead. The macro-dipole moment along the stacking direction for this oligomer was found to be 8.22 D. The time evolution of the number of aggregates and their sizes are presented in Figure S6, which was obtained through a cluster analysis.

It should be borne in mind that the dynamics in CG representation is typically much faster[47] than in the AA one due to the softer and smoother potentials employed. Hence, the CG time scales observed here need to be stretched to compare against realistic ones.

Dynamic Equilibrium between Molecules of Different Stacks. Self-assembly of disc shaped C_3-symmetric molecules obey the "sergeants-and-soldiers"[33] principle. Oligomers of achiral molecules do not exhibit any specific handedness, i.e., an equal proportion of P and M enantiomers exist in solution. Introduction of a small amount of chiral molecules (sergeants) into such a solution of achiral (soldiers) molecules induces a specific handedness to the supramolecular polymer. Such a solution exhibits a circular dichroism (CD) signal in accordance with the nature of the added sergent molecules. Recently, Meijer and co-workers[48] showed that a mixture of two separate fibers labeled with different dyes could not be distinguished after 24 h. This process of mixing proceeds neither through *polymerization-depolymerization* nor by *fragmentation-recombination* and was accounted for by the dynamic exchange of molecules between the oligomers.

We would like to understand the phenomenon of exchange of monomers using MD simulations and estimate the FE change associated with this process. Toward this aim, a simulation box consisting of a preformed oligomer of size 20 soaked in 12 834 *n*-nonane molecules was constructed. Steered molecular dynamics (SMD)[49,50] simulations were carried out in the isothermal−isobaric (NPT) ensemble to determine the FE change for the removal of a molecule from this oligomer into the bulk solution. SMD is a nonequilibrium method in which accumulation of work as a function of the extent of steering can be determined. However, the FE difference is an equilibrium quantity that can be obtained from several nonequilibrium trajectories using the Jarzynski equality.[51] In our simulations, the SMD spring constant was chosen to be 100 kcal/mol/Å^2, and SMD calculations were performed in constant velocity mode at various pulling rates. The reaction coordinate (RC) was defined as the distance between the center of BZ beads of molecule 11, and the mean position obtained from BZ beads of molecules 10 and 12 (see Figure 6a). "Distance" style was employed to remove a molecule from the stack. The entire stack, other than molecule 11, was restricted within a parallelepiped so as to preserve its columnar structure during the evolution of the RC. The converged FE profile, shown in Figure 6b, was obtained using Jarzynski's equality,[51] averaged over 30 SMD profiles. The individual nonequilibrium work

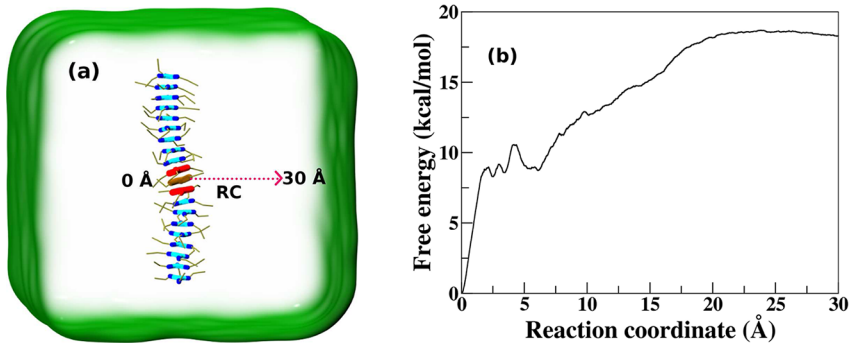

Figure 6. (a) Schematic representation of the reaction coordinate (RC) for pulling a molecule from the middle of a 20-mer stack into bulk solution. Molecules 10 and 12 are shown in red, and molecule 11 is represented in brown. (b) Free energy profile averaged using Jarzynski's equality over 30 SMD work trajectories. Simulations were carried out using Model B at a temperature of 298.15 K.

DOI: 10.1021/acs.jpcb.5b01655
J. Phys. Chem. B 2015, 119, 5738−5746

profiles from SMD are shown in Figure S7. The molecule in the center of the stack is stabilized by 18.2 kcal/mol compared to its monomeric state in bulk solution. When a monomer in bulk solution approaches the core of an oligomer, the FE gradually decreases up to a distance of 4 Å. The profile at shorter distances is rugged and exhibits small barriers. This is due to the adoption of various orientations that the molecule inserting itself into the oligomer takes. The only possibility for a monomer to incorporate itself within the core of the stack is by keeping its benzene plane parallel to the molecules that are part of the oligomer. Since the barriers are only around 1−2 kcal/mol, this process is indeed accessible to thermal energy at ambient conditions. This observation implies that a molecule in the center of the stack can indeed exchange with the pool of monomers in the bulk solution.[33]

Nature of Cooperativity and Critical Size of the Nucleus. BTA monomers present in a high-temperature solution self-assemble upon slow cooling via the formation of a nucleus. The nucleus formation can be associated either with lowering the free energy (downhill) or an increase (uphill) with respect to monomers.[52] It is challenging to distinguish the two experimentally. For a better understanding of the experiments, analytical models[53,54] have been developed by assuming the nucleus size to be 2 (i.e., a dimer). Such models form the basis to evaluate thermodynamic properties and determine the self-assembly mechanism. We are thus curious to find out (i) the nature of cooperativity: downhill or uphill, and (ii) the size of the nucleus.

From a theoretical point of view, the free energy of formation of an oligomer (from monomers) as a function of its size determines the mechanism of polymerization.[52] In our earlier work employing an all-atom model,[7] ABF simulations were used to demonstrate cooperativity in the FE for the removal of a molecule from an oligomer. The RC was defined as the distance between the center of mass of BZ beads of two outermost molecules, hydrogen bonded to each other (see Figure 7a). In these simulations, RC was divided into bins of 0.1 Å, in each of which the force experienced on it was averaged over 500 steps. The entire RC was divided into two nonoverlapping windows spanning the distance from 3 to25 Å. "Distance" colvar style was employed to determine the FE along the RC. BZ beads of molecule 2 were fixed to define a coaxial cylinder of radius 3 Å using "distanceXY" along the *z*-axis, and molecule 1 was restricted in the cylinder (see Figure 7 for definition of molecule indices). Two sets of simulations were carried out by modeling BTA either with Model A or Model B. All the simulations were performed for at least 100 ns to obtain converged FE profiles, and the same are displayed in Figure 7b,c. The ratio of maximum to minimum samples collected across the RC was ≈8. The free energy of binding of a monomer to an oligomer increases gradually from a dimer to a tetramer, beyond which it converges to a value around 16 kcal/mol. Besides the exhibition of self-assembly from dispersed monomers, cooperativity in FE is another important validation for the CG models developed here.

Irrespective of whether a molecule from solution adds to the end of a stack or to its middle, the free energy change should be the same. Thus, the difference in the FE changes reported here for the end-addition (around 16 kcal/mol) and the addition to the center (around 18 kcal/mol) should be seen as nominal and likely to arise from sampling and methodological differences.

In general, apart from a monomer, a short oligomer too can add to a pre-existing stack on the latter's terminal. We have studied the free energy change involved in this process as a function of the size of the short oligomer, using the ABF method. Once again, the "DistanceZ" style was employed in determining the change in FE, and RC was defined as the distance between the center of the short oligomer (n = 2,3,5,7) and the closest molecule in the stack.[55] BZ beads of the closest molecule were fixed to define a coaxial cylinder along z-axis. Table 2 shows the corresponding FE differences. While the monomer joins a stack (19-mer) with a free energy gain of

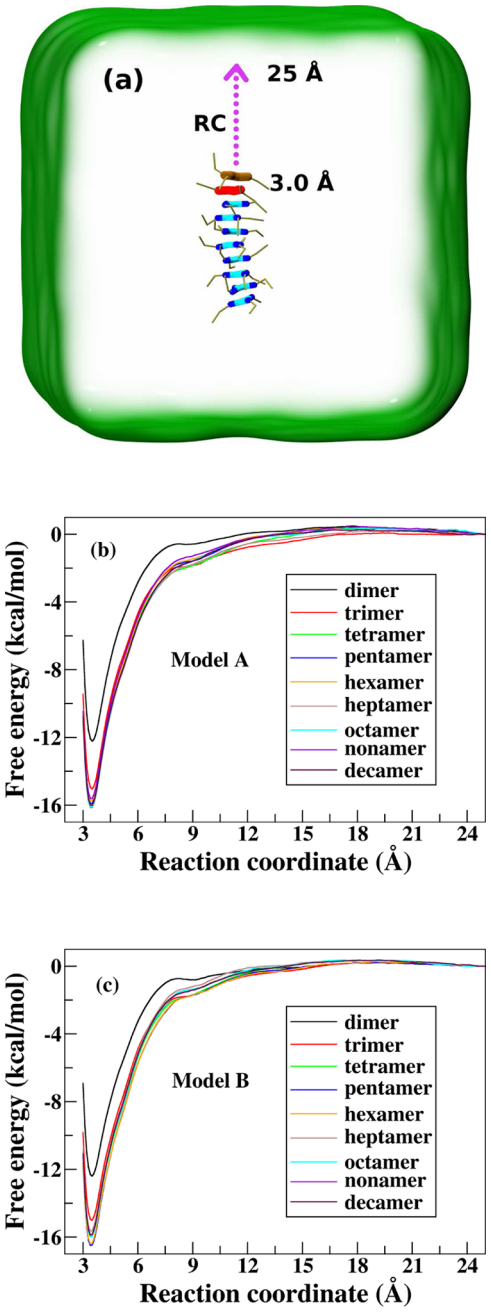

Figure 7. (a) Schematic representation of RC for removing a molecule from one end of the stack. RC is the distance between the centers of mass of the molecule being removed and the one that is closest to it present in the oligomer. Molecule 1 is shown in brown, and molecule 2 is represented in red. (b,c) Free energy profiles associated with the process of removing a molecule from oligomers of various sizes, each solvated in *n*-nonane solution at 298.15 K using Model A and Model B, respectively.

DOI: 10.1021/acs.jpcb.5b01655
J. Phys. Chem. B 2015, 119, 5738−5746

Table 2. Free Energy Change for the Removal of an Oligomer from the Terminus of a Stack into Bulk Solution at 298.15 K Using Model B[a]

oligomer	ΔG (kcal/mol)
monomer	15.92
dimer	19.76
trimer	21.50
pentamer	21.44
heptamer	21.67

[a]The total number of molecules in the stack is 20.

around 16 kcal/mol, a dimer is seen to add to a 18-mer with a FE gain of around 20 kcal/mol. This FE change remains more or less at the same value for larger oligomers fusing with a stack. The change in FE between a monomer addition and a dimer addition to a pre-existing stack further points to cooperativity in self-assembly.

In the following, G_n denotes the free energy of a n-mer in solution. The free energy of formation of a n-mer out of n individual monomers is denoted as ΔG_n. It is challenging to determine this quantity directly, which may involve the effective use of the coordination number as a reaction coordinate. However, the results obtained so far can themselves be used to determine ΔG_n. We illustrate this procedure through the free energy of formation of a trimer from three monomers in solution ($\Delta G_3 = G_3 - 3G_1$) in the following manner:

1. Two out of the three dispersed molecules can form a dimer, and the free energy change associated with this process is dimerization free energy (DFE), which has been determined earlier ($\Delta G_2 = G_2 - 2G_1$).
2. A third molecule can bind to the dimer, and the free energy change for this process can be quantified by the reverse process—that of removing a molecule from a trimer ($G_3 - G_2 - G_1$), as discussed above.

The FE of a trimer with respect to the three monomers (ΔG_3) can be simply obtained by adding the above two quantities. The FE of formation for oligomers ($\Delta G_n = G_n - nG_1$) of different sizes (n) were determined likewise and are presented in Figure 8. The trend is similar to what was delineated for downhill cooperativity in ref 52. Prior to the formation of the nucleus, the change in the formation FE for an oligomer increases but attains a constant value beyond the point of nucleation. During the elongation process, monomers attach to an oligomer with the same binding strength (association constant). Clearly, the trimer appears to be the likely nucleus, beyond which size the change in FE per molecule converges to a value of around 16 kcal/mol. In BTA systems, a n-mer possesses $3(n-1)$ hydrogen bonds. Thus, the ratio of the free energy of formation of a n-mer (ΔG_n) to the number of triplets of hydrogen bonds present in the stack provides information on the stabilization of a molecule via not only the H-bonds it forms with its neighbors, but also through long-range interactions it is involved in. Such a quantity is displayed in Figure 9. $\Delta G_n/(n-1)$ increases with oligomer size (n) until saturation, which is a signature of cooperativity in the self-assembly of BTA molecules.

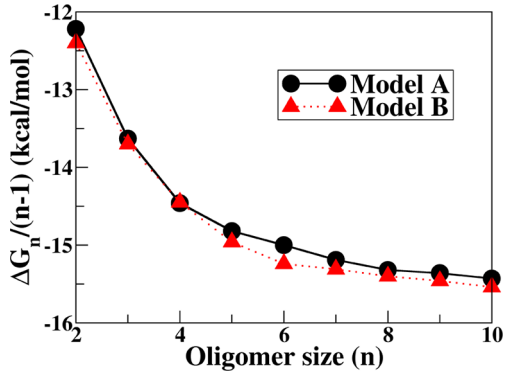

Figure 9. Free energy of formation of an oligomer from individual monomers, normalized per contact ($\Delta G_n/(n-1)$). Both models predict a cooperative nature of self-assembly of BTA molecules.

CONCLUSIONS

We have developed two CG models (Models A and B) for benzene-1,3,5-tricarboxamide that have exhibited a good potential for the study of self-assembly of BTA in an apolar, n-nonane solvent. Intramolecular potential terms in the coarse grain representation have been fitted to either a harmonic form (for unimodal distributions) or to tabulated potentials (for bimodal ones). A short-range potential is employed to capture hydrogen bonding interactions. In Model B, an intrinsic point dipole is introduced on one of the CG beads to represent the dipole moment of the intermolecular hydrogen bond. Consequently, a BTA stack acquires a macro-dipole along the

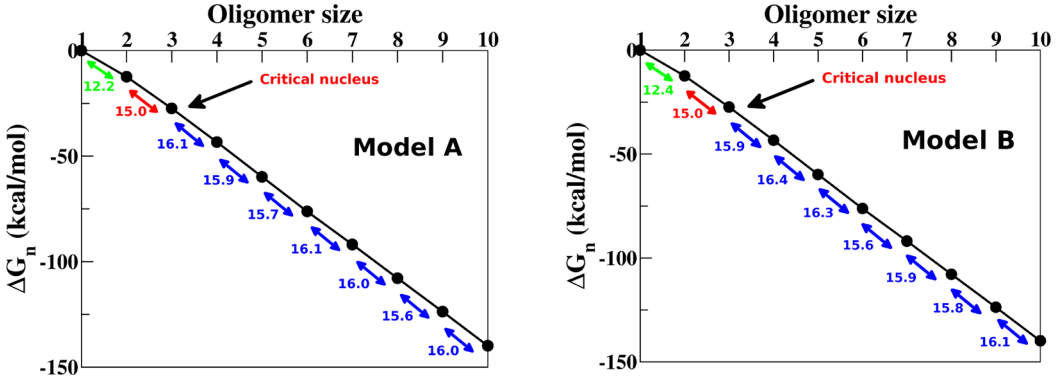

Figure 8. Free energy of formation ($\Delta G_n = G_n - nG_1$) for various sizes of oligomers in n-nonane solution at 298.15 K. The difference in FE of formation between oligomers differing by one molecule ($\Delta G_n - \Delta G_{n-1}$) are written as text within the figure. The critical size of the nucleus is identified as a trimer.

DOI: 10.1021/acs.jpcb.5b01655
J. Phys. Chem. B 2015, 119, 5738−5746

stacking direction. Dimerization and solvation FE profiles obtained from AA simulations were reproduced using both the CG models. The stability of asymmetric stacking (2:1) over a symmetric one (3:0) was also demonstrated using Model-B.[7] Both the CG models predict the self-assembly of molecules from a dispersed configuration to form one-dimensional aggregates with nearly quantitative structural characteristics. The free energies of oligomerization for the models are comparable to each other. However, Model B is preferred over Model A due to the former's capability to exhibit a macrodipole moment for the oligomer. The same could be vital in modeling microscopic phenomena associated with ferroelectric loop experiments of BTA samples.[56,57]

A series of steered MD simulations were performed to determine the free energy change in removing a molecule from the center of a stack. A monomer in the core of an oligomer is stabilized by ≈18 kcal/mol with respect to its dispersed state in bulk solvent. These simulations demonstrate the feasibility of monomer exchange between the stacks and the bath of monomers in solution, which forms the basis of a principle called sergeants-and-soldiers[33] in the domain of supramolecular polymers. ABF simulations yielded rich details on the cooperativity in FE in the binding of a molecule to oligomers of various sizes. A molecule is more strongly bound to longer oligomers than to smaller ones. These FE calculations also demonstrate that polymerization in these systems is one of downhill cooperativity and that the size of the nucleus is more likely to be three rather than two.[53,54]

The approach presented in this article can be adopted for many molecules being investigated in the domain of supramolecular polymer chemistry.[58] These will constitute our future endeavors. In particular, the sticky dipole approach has not been explored much in molecular systems, and we hope that the current work will motivate more efforts in this direction. Although the model developed here is specific for BTA with hexyl tail, it is applicable to systems with other lengths of alkyl tail. This aspect encourages us to study the effects of varying alkyl tail lengths on the aggregate morphology. Modifications in the molecule such as the addition of different functionalities, linkers, and the self-assembling moiety can, in principle, be modeled using the procedure followed here. It may also be pertinent to develop much simpler models that incorporate solvent effects implicitly.

■ ASSOCIATED CONTENT

Supporting Information

Force field parameters for both the CG models are provided (Table S1 and S2). Comparison of the intramolecular distributions of AA and CG are shown. Snapshots illustrating the self-assembly of BTA in explicit *n*-nonane within CG models are provided. This material is available free of charge via the Internet at http://pubs.acs.org.

■ AUTHOR INFORMATION

Corresponding Author

*E-mail: bala@jncasr.ac.in.

Notes

The authors declare no competing financial interest.

■ ACKNOWLEDGMENTS

K.K.B. thanks CSIR, India for a senior research fellowship. S.B. thanks Sheikh Saqr Laboratory, JNCASR, for a senior fellowship. We thank DST, India for support. The authors gratefully acknowledge several insightful discussions with Prof. Subi J. George and Chidambar Kulkarni. Chidambar Kulkarni is also thanked for comments on an earlier version of this manuscript.

■ REFERENCES

(1) Tovar, J. D. Supramolecular Construction of Optoelectronic Biomaterials. *Acc. Chem. Res.* **2013**, *46*, 1527−1537.
(2) Cantekin, S.; de Greef, T. F. A.; Palmans, A. R. A. Benzene-1,3,5-tricarboxamide: A Versatile Ordering Moiety for Supramolecular Chemistry. *Chem. Soc. Rev.* **2012**, *41*, 6125−6137.
(3) Smulders, M. M. J.; Schenning, A. P. H. J.; Meijer, E. W. Insight into the Mechanisms of Cooperative Self-Assembly: The "Sergeants-and-Soldiers" Principle of Chiral and Achiral C3-Symmetrical Discotic Triamides. *J. Am. Chem. Soc.* **2008**, *130*, 606−611.
(4) Stals, P. J. M.; Smulders, M. M. J.; Martín-Rapún, R.; Palmans, A. R. A.; Meijer, E. W. Asymmetrically Substituted Benzene-1,3,5-tricarboxamides: Self-Assembly and Odd-Even Effects in the Solid State and in Dilute Solution. *Chem.—Eur. J.* **2009**, *15*, 2071−2080.
(5) Filot, I. A. W.; Palmans, A. R. A.; Hilbers, P. A. J.; van Santen, R. A.; Pidko, E. A.; de Greef, T. F. A. Understanding Cooperativity in Hydrogen-Bond-Induced Supramolecular Polymerization: A Density Functional Theory Study. *J. Phys. Chem. B* **2010**, *114*, 13667−13674.
(6) Kulkarni, C.; Reddy, S. K.; George, S. J.; Balasubramanian, S. Cooperativity in the Stacking of Benzene-1,3,5-tricarboxamide: The Role of Dispersion. *Chem. Phys. Lett.* **2011**, *515*, 226−230.
(7) Bejagam, K. K.; Fiorin, G.; Klein, M. L.; Balasubramanian, S. Supramolecular Polymerization of Benzene-1,3,5-tricarboxamide: A Molecular Dynamics Simulation Study. *J. Phys. Chem. B* **2014**, *118*, 5218−5228.
(8) Kulkarni, C.; Balasubramanian, S.; George, S. J. What Molecular Features Govern the Mechanism of Supramolecular Polymerization? *ChemPhysChem* **2013**, *14*, 661−673.
(9) Wegner, M.; Dudenko, D.; Sebastiani, D.; Palmans, A. R. A.; de Greef, T. F. A.; Graf, R.; Spiess, H. W. The Impact of the Amide Connectivity on the Assembly and Dynamics of Benzene-1,3,5-tricarboxamides in the Solid State. *Chem. Sci.* **2011**, *2*, 2040−2049.
(10) Stals, P. J. M.; Haveman, J. F.; Martin-Rapun, R.; Fitie, C. F. C.; Palmans, A. R. A.; Meijer, E. W. The Influence of Oligo(ethylene glycol) Side Chains on the Self-assembly of Benzene-1,3,5-tricarboxamides in the Solid State and in Solution. *J. Mater. Chem.* **2009**, *19*, 124−130.
(11) Matsunaga, Y.; Nakayasu, Y.; Sakai, S.; Yonenaga, M. Liquid Crystal Phases Exhibited by *N*,*N*′,*N*″-Trialkyl-1,3,5-Benzenetricaboxamides. *Mol. Cryst. Liq. Cryst.* **1986**, *141*, 327−333.
(12) Singer, J. C.; Giesa, R.; Schmidt, H.-W. Shaping Self-assembling Small Molecules into Fibres by Melt Electrospinning. *Soft Matter* **2012**, *8*, 9972−9976.
(13) Stals, P. J. M.; Korevaar, P. A.; Gillissen, M. A. J.; de Greef, T. F. A.; Fitié, C. F. C.; Sijbesma, R. P.; Palmans, A. R. A.; Meijer, E. W. Symmetry Breaking in the Self-Assembly of Partially Fluorinated Benzene-1,3,5-tricarboxamides. *Angew. Chem., Int. Ed.* **2012**, *51*, 11297−11301.
(14) Wang, F.; Gillissen, M. A. J.; Stals, P. J. M.; Palmans, A. R. A.; Meijer, E. W. Hydrogen Bonding Directed Supramolecular Polymerisation of Oligo(Phenylene-Ethynylene)s: Cooperative Mechanism, Core Symmetry Effect and Chiral Amplification. *Chem.—Eur. J.* **2012**, *18*, 11761−11770.
(15) Ishioka, Y.; Minakuchi, N.; Mizuhata, M.; Maruyama, T. Supramolecular Gelators Based on Benzenetricarboxamides for Ionic Liquids. *Soft Matter* **2014**, *10*, 965−971.
(16) Jung, S. H.; Jeon, J.; Kim, H.; Jaworski, J.; Jung, J. H. Chiral Arrangement of Achiral Au Nanoparticles by Supramolecular Assembly of Helical Nanofiber Templates. *J. Am. Chem. Soc.* **2014**, *136*, 6446−6452.
(17) Smulders, M. M. J.; Buffeteau, T.; Cavagnat, D.; Wolffs, M.; Schenning, A. P. H. J.; Meijer, E. W. C3-symmetrical Self-assembled

DOI: 10.1021/acs.jpcb.5b01655
J. Phys. Chem. B 2015, 119, 5738−5746

Structures Investigated by Vibrational Circular Dichroism. *Chirality* **2008**, *20*, 1016−1022.
(18) Albuquerque, R. Q.; Timme, A.; Kress, R.; Senker, J.; Schmidt, H.-W. Theoretical Investigation of Macrodipoles in Supramolecular Columnar Stackings. *Chem.—Eur. J.* **2013**, *19*, 1647−1657.
(19) Nakano, Y.; Hirose, T.; Stals, P. J. M.; Meijer, E. W.; Palmans, A. R. A. Conformational Analysis of Supramolecular Polymerization Processes of Disc-like Molecules. *Chem. Sci.* **2012**, *3*, 148−155.
(20) Nakano, Y.; Markvoort, A. J.; Cantekin, S.; Filot, I. A. W.; ten Eikelder, H. M. M.; Meijer, E. W.; Palmans, A. R. A. Conformational Analysis of Chiral Supramolecular Aggregates: Modeling the Subtle Difference between Hydrogen and Deuterium. *J. Am. Chem. Soc.* **2013**, *135*, 16497−16506.
(21) Karimi-Varzaneh, H. A.; van der Vegt, N. F. A.; Müller-Plathe, F.; Carbone, P. How Good Are Coarse-Grained Polymer Models? A Comparison for Atactic Polystyrene. *ChemPhysChem* **2012**, *13*, 3428−3439.
(22) Shinoda, W.; Discher, D. E.; Klein, M. L.; Loverde, S. M. Probing the Structure of PEGylated-lipid Assemblies by Coarse-grained Molecular Dynamics. *Soft Matter* **2013**, *9*, 11549−11556.
(23) Prasitnok, K.; Wilson, M. R. A Coarse-grained Model for Polyethylene Glycol in Bulk Water and at a Water/air Interface. *Phys. Chem. Chem. Phys.* **2013**, *15*, 17093−17104.
(24) Kawamoto, S.; Shinoda, W. Free Energy Analysis along the Stalk Mechanism of Membrane Fusion. *Soft Matter* **2014**, *10*, 3048−3054.
(25) Nawaz, S.; Carbone, P. Coarse-Graining Poly(ethylene oxide)-Poly(propylene oxide)-Poly(ethylene oxide) (PEO-PPO-PEO) Block Copolymers Using the MARTINI Force Field. *J. Phys. Chem. B* **2014**, *118*, 1648−1659.
(26) Klein, M. L.; Shinoda, W. Large-Scale Molecular Dynamics Simulations of Self-Assembling Systems. *Science* **2008**, *321*, 798−800.
(27) Samanta, S. K.; Bhattacharya, S.; Maiti, P. K. Coarse-Grained Molecular Dynamics Simulation of the Aggregation Properties of Multiheaded Cationic Surfactants in Water. *J. Phys. Chem. B* **2009**, *113*, 13545−13550.
(28) Mondal, J.; Mahanthappa, M.; Yethiraj, A. Self-Assembly of Gemini Surfactants: A Computer Simulation Study. *J. Phys. Chem. B* **2013**, *117*, 4254−4262.
(29) Schor, M.; Ensing, B.; Bolhuis, P. G. A Simple Coarse-grained Model for Self-Assembling Silk-like Protein Fibers. *Faraday Discuss.* **2010**, *144*, 127−141.
(30) Shinoda, W.; DeVane, R.; Klein, M. L. Multi-property Fitting and Parameterization of a Coarse Grained Model for Aqueous Surfactants. *Mol. Simul.* **2007**, *33*, 27−36.
(31) Bhargava, B. L.; Devane, R.; Klein, M. L.; Balasubramanian, S. Nanoscale Organization in Room Temperature Ionic Liquids: A Coarse Grained Molecular Dynamics Simulation Study. *Soft Matter* **2007**, *3*, 1395−1400.
(32) DeVane, R.; Klein, M. L.; Chiu, C.-c.; Nielsen, S. O.; Shinoda, W.; Moore, P. B. Coarse-Grained Potential Models for Phenyl-Based Molecules: I. Parametrization Using Experimental Data. *J. Phys. Chem. B* **2010**, *114*, 6386−6393.
(33) Palmans, A. R. A.; Vekemans, J. A. J. M.; Havinga, E. E.; Meijer, E. W. Sergeants-and-Soldiers Principle in Chiral Columnar Stacks of Disc-Shaped Molecules with C3 Symmetry. *Angew. Chem., Int. Ed.* **1997**, *36*, 2648−2651.
(34) Stockmayer, W. H. Second Virial Coefficients of Polar Gases. *J. Chem. Phys.* **1941**, *9*, 398−402.
(35) Bartke, J.; Hentschke, R. Phase Behavior of the Stockmayer Fluid via Molecular Dynamics Simulation. *Phys. Rev. E* **2007**, *75*, 061503.
(36) Orsi, M. Comparative Assessment of the ELBA Coarse-grained Model for Water. *Mol. Phys.* **2014**, *112*, 1566−1576.
(37) Orsi, M.; Essex, J. W. Physical Properties of Mixed Bilayers Containing Lamellar and Nonlamellar Lipids: Insights from Coarse-grain Molecular Dynamics Simulations. *Faraday Discuss.* **2013**, *161*, 249−272.
(38) Nosé, S. A. Unified Formulation of the Constant Temperature Molecular Dynamics Methods. *J. Chem. Phys.* **1984**, *81*, 511−519.
(39) Hoover, W. G. Canonical Dynamics: Equilibrium Phase-space Distributions. *Phys. Rev. A* **1985**, *31*, 1695−1697.
(40) Schneider, T.; Stoll, E. Molecular-dynamics Study of a Three-dimensional One-component Model for Distortive Phase Transitions. *Phys. Rev. B* **1978**, *17*, 1302−1322.
(41) Plimpton, S. Fast Parallel Algorithms for Short-Range Molecular Dynamics. *J. Comput. Phys.* **1995**, *117*, 1−19.
(42) Fiorin, G.; Klein, M.; Hénin, J. Using Collective Variables to Drive Molecular Dynamics Simulations. *Mol. Phys.* **2013**, *111*, 3345−3362.
(43) Humphrey, W.; Dalke, A.; Schulten, K. VMD - Visual Molecular Dynamics. *J. Mol. Graphics* **1996**, *14*, 33−38.
(44) Jmol: An open-source Java viewer for chemical structures in 3D. http://www.jmol.org/ (accessed Apr 2, 2015).
(45) Darve, E.; Rodríguez-Gómez, D.; Pohorille, A. Adaptive Biasing Force Method for Scalar and Vector Free Energy Calculations. *J. Chem. Phys.* **2008**, *128*, 144120.
(46) Martínez, L.; Andrade, R.; Birgin, E. G.; Martínez, J. M. PACKMOL: A Package for Building Initial Configurations for Molecular Dynamics Simulations. *J. Comput. Chem.* **2009**, *30*, 2157−2164.
(47) Diffusion coefficients were determined from AA and CG simulations of one BTA in 500 *n*-nonane molecules at 298.15 K. D_{AA} = 1.68 × 10^{-7} cm^2 s^{-1} and D_{CG} = 34.26 × 10^{-7} cm^2 s^{-1}.
(48) Albertazzi, L.; van der Zwaag, D.; Leenders, C. M. A.; Fitzner, R.; van der Hofstad, R. W.; Meijer, E. W. Probing Exchange Pathways in One-Dimensional Aggregates with Super-Resolution Microscopy. *Science* **2014**, *344*, 491−495.
(49) Park, S.; Khalili-Araghi, F.; Tajkhorshid, E.; Schulten, K. Free Energy Calculation from Steered Molecular Dynamics Simulations Using Jarzynski's Equality. *J. Chem. Phys.* **2003**, *119*, 3559−3566.
(50) Park, S.; Schulten, K. Calculating Potentials of Mean Force from Steered Molecular Dynamics Simulations. *J. Chem. Phys.* **2004**, *120*, 5946−5961.
(51) Jarzynski, C. Nonequilibrium Equality for Free Energy Differences. *Phys. Rev. Lett.* **1997**, *78*, 2690−2693.
(52) De Greef, T. F. A.; Smulders, M. M. J.; Wolffs, M.; Schenning, A. P. H. J.; Sijbesma, R. P.; Meijer, E. W. Supramolecular Polymerization. *Chem. Rev.* **2009**, *109*, 5687−5754.
(53) Jonkheijm, P.; van der Schoot, P.; Schenning, A. P. H. J.; Meijer, E. W. Probing the Solvent-Assisted Nucleation Pathway in Chemical Self-Assembly. *Science* **2006**, *313*, 80−83.
(54) Markvoort, A. J.; ten Eikelder, H. M. M.; Hilbers, P. A. J.; de Greef, T. F. A.; Meijer, E. W. Theoretical Models of Nonlinear Effects in Two-Component Cooperative Supramolecular Copolymerizations. *Nat. Commun.* **2011**, *2*, 509.
(55) RMSD was used as the colvar variable to restrain the geometry of the oligomer.
(56) Fitié, C. F. C.; Roelofs, W. S. C.; Kemerink, M.; Sijbesma, R. P. Remnant Polarization in Thin Films from a Columnar Liquid Crystal. *J. Am. Chem. Soc.* **2010**, *132*, 6892−6893.
(57) Fitié, C. F. C.; Roelofs, W. S. C.; Magusin, P. C. M. M.; Wübbenhorst, M.; Kemerink, M.; Sijbesma, R. P. Polar Switching in Trialkylbenzene-1,3,5-tricarboxamides. *J. Phys. Chem. B* **2012**, *116*, 3928−3937.
(58) Jain, A.; George, S. J. New Directions in Supramolecular Electronics. *Mater. Today* **2015**, DOI: 10.1016/j.mattod.2015.01.015.

DOI: 10.1021/acs.jpcb.5b01655
J. Phys. Chem. B 2015, 119, 5738−5746